Defining coiling adiabaticity

Sylvain O'Reilly, Benoit Sévigny, Bertrand Gauvreau
ITF Laboratories, 400 Montpellier Blvd., Montréal, Québec, H4N 2G7 Canada

ABSTRACT

Most common high power fiber lasers use large mode area (LMA) fiber to reduce unwanted non-linearity. Such fibers usually guide few modes but operate close to single mode regime (underfill condition) for best beam quality. For packaging considerations or for high order mode filtering, coiling the gain fiber is mandatory. Determining the best coiling architecture may look simple but extra care must be taken when dealing with few moded LMA fiber.

We present a formalism to quantitatively express the adiabaticity of an optical fiber coil based on the normalized coupling coefficient betweens modes. The goal is to evaluate the capability of a coiling system to preserve the modal repartition of the optical intensity and preserve beam quality at fiber output. We present typical coiling configurations as examples.

A simple interferometric measurement setup is proposed to study figures of merit of a coil.

Keywords: Fiber coiling, adiabaticity, fiber laser

1. INTRODUCTION

The necessity of coiling fiber for integration of high power fiber laser has led to questioning about the figures of merit of such a coil. It is known that fiber guiding parameters have a significant impact on losses and beam quality at output of the fiber. The present article aims at quantifying the adiabaticity of coils, meaning the capability of a coiled system to preserve the modal repartition of the optical intensity throughout the coil.

The adabiatic condition over the normalized variation of bend radius can be written similarly as for adiabaticity in tapered fibers. Basically, it is a quantitative comparison between coupling length of the first two modes and phase beatlength. We show that in order to preserve adiabaticity, a fiber coil has to show smooth variations of its radius of curvature.

A simple setup for characterization is proposed. A large mode area (LMA) fiber is coiled between mode field adapters (MFA). Single mode fiber is put at both ends so injection is made only in LP_{01}. As LP_{01} and LP_{11} have different effective index of refraction, it results in an interferometer in which the spectral fringes visibility scales with the coupling between the first modes. Therefore, it can be used as a characterization setup to compare adiabaticity between various coil configurations.

2. ADIABATICITY DEFINITION

The adiabaticity will be defined as a quantitative comparison between coupling length between first two modes and beat length of these modes in the studied coiled. The coupling length is defined as:

$$L_C = \frac{2\pi}{C_{12}} \tag{1}$$

The coupling coefficient is defined in terms of local modes approximation:

$$C_{12} = -i\frac{k^2}{2\sqrt{|\beta_1\beta_2|}}\frac{1}{\beta_1 - \beta_2}\int_{A_\infty}\frac{\partial n^2}{\partial z}\hat{\psi_1^*}\hat{\psi_2}dA \tag{2}$$

where k is the wave number, β_i is the propagation constant of the i mode, $\hat{\psi_i}$ is the normalized field of the i mode, n is the index of refraction, z is the longitudinal position and A is the fiber's cross-section.

We can also define a beat length between two local modes in regard of their propagation constant:

$$z_b = \frac{2\pi}{\beta_1 - \beta_2} \tag{3}$$

The perturbed index of refraction in a bent fiber can be expressed as [1]:

$$n = n_0 \left(1 + \frac{x}{R_{eff}}\right) \tag{4}$$

where x is the coordinate from the center of the fiber, n_0 is the effective refraction index of the mode in a straight piece of fiber, $R_{eff} = 1.27R$ is the effective bending radius [1] and R is the coiling radius. To calculate the coupling coefficient one has to express:

$$\frac{\partial n^2}{\partial z} = -2n_0^2 \frac{x}{R_{eff}} \left(\frac{1}{R}\frac{\partial R}{\partial z}\right) \tag{5}$$

The higher order term was neglected. One can express coupling in terms of normalized coupling coefficient $\underline{C}_{12}$:

$$C_{12} = \underline{C}_{12} \left(\frac{1}{R}\frac{\partial R}{\partial z}\right) \tag{6}$$

The quantity to be studied is the normalized variation of bend radius that can be written:

$$\rho_0 = \left(\frac{1}{R}\frac{\partial R}{\partial z}\right) \tag{7}$$

A similar criterion is used while evaluating adiabaticity of a tapered fiber [2]. In such structures, one will evaluate the rate of change in the inverse taper ratio (ITR) and define the adiabaticity criteria to be $\rho = 1$, which is considered to be the border between adiabatic and non-adiabatic regime. When considering fiber coiling though, conditions have to be more stringent. For instance, having the coupling length the same order of magnitude as the beatlength of the modes would result in a very efficient coupler from LP_{01} to LP_{11} which is precisely what is to be avoided. Therefore, one has to look at orders of magnitude under the nominal value of ρ_0. This can be wirtten

$$\rho \ll \frac{\beta_1 - \beta_2}{\underline{C}_{12}} \tag{8}$$

3. SIMULATION

One can solve the first modes in a bent fiber in order to plot adiabaticity curves. The method used to solve modes was the shift-invert matrix resolution [3]. Doing so, we obtain the mode profiles that are fed into equation 2.

As the fiber is bent further, the electrical field centroid is slightly shifted and the coupling coefficient changes. As a reference, figure 2 shows the modes with a bend radius of about 5 cm. One can see the slighly deformed LP_{11} mode. LP_{01} mode is also, but imperceptibly stretched.

4. EXPERIMENTATION

A simple set-up for characterization is proposed. A large mode area (LMA) fiber is coiled between mode field adapters (MFA) such as light coming from single mode fiber (SMF) is launched in LP_{01}. The modal coupling occurs in the coil under test (CUT) and the remaining of LP_{01} is extracted with a MFA and guided in an output in SMF. The spectrum is recovered with an optical spectrum analyser (OSA).

We study here 4 shapes of coil under test: 1- circular coil including relatively straight approach to the coil; 2- smoothed approach circular coil; 3- figure of eight shaped coil and 4- kidney shaped coil. The path taken by the fibers are shown on figure 4. The data are shown on table 1. We included in the circular coils the approach of the fiber since that is where all coupling takes place and this is how 2 distinct circular coils will differentiate one another. On kidney and 8 shape coils, the approaches were not considered, the point being to study a particular coiling geometry. For reference, on kidney shape coil, the entrance and exit were tangeant to the biggest radius of curvature of the coil (bottom region on figure 12). On the 8 shape coil the entrance was at the inflexion point, while the exit was tangeant to one of lobes and parallel to the

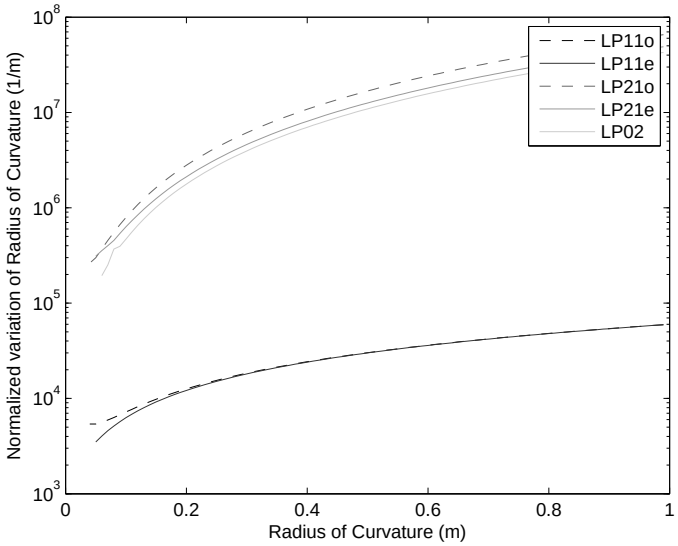

Figure 1. First modes adiabaticity curves. The only modes suscpetible to couple to LP_{01} are LP_{11} modes. As one can see, Degeneracy is lifted on orthogonal LP_{11} modes when the fiber is tightly bent. Numerical noise near smaller radius region appears when the modes cease to be guided by the core.This is a basically the cut-off of the mode. The fiber used in this simulation was 30/250 with a numerical apperture of 0.06. The wavelength was set at 1060 nm.

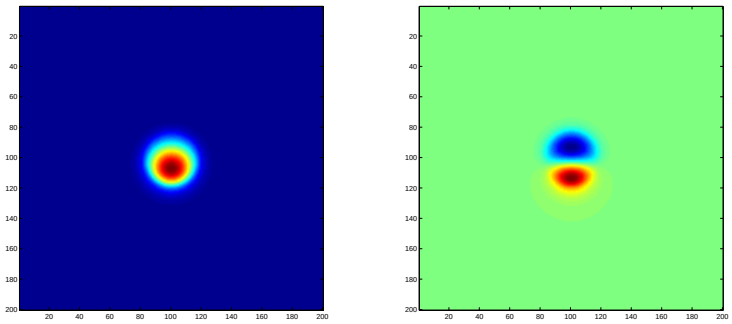

Figure 2. Two first modes susceptibles to couple: On left, LP_{01}; On right, LP_{11}.

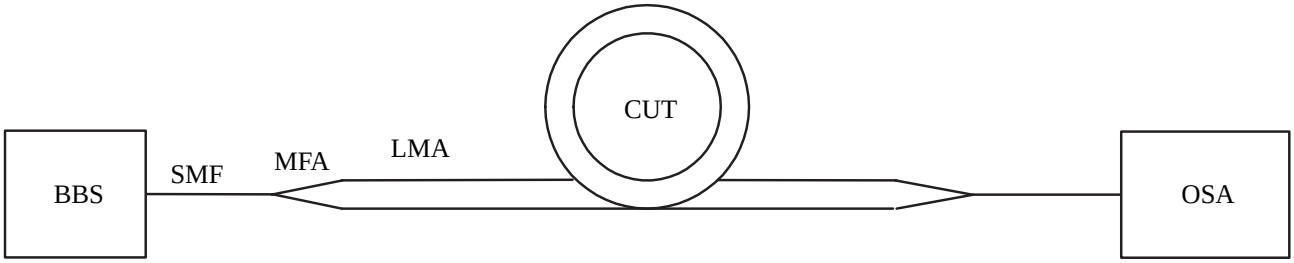

Figure 3. Experimental set-up. BBS: Broad band source, SMF: Single Mode Fiber, MFA: Mode Field Adapter, LMA: Large Mode Area, CUT: Coil Under Test, OSA: optical Spectrum Analyser.

Coil type	Total length (cm)	# turns	footprint (cm^2)
Single coil	151	7.5	41
8 shape coil	169	$\approx 2\frac{2}{3}$	98
Kidney shape coil	178	4	128
Smoothed Approach Single Coil	174	7.5	58

Table 1. Experimental parameters of coils under test. The footprint is defined as the area of the smallest rectangle containing the coil. Fiber used for the experiment is 30/250 with a numerical apperture of 0.06.

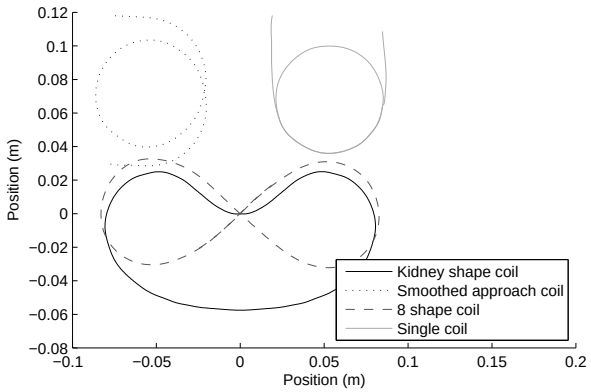

Figure 4. The four studied coils one over the other. We preserved as much as possible the minimum radius of curvature and fiber length. Footprint and number of turn were kept variable under different coil geometries.

entrance. On the smoothed approach single coil, the constraints on the bend radius were relieved so the local bend radius was changing from 60 to 71 mm. This was done so in order to see if less constrained fiber was showing a more adiabatic behavior. This was however cumbersome to model or measure so only the approaches and a single turn were considered.

5. DISCUSSION

The adiabaticity criterion is useful to study how smooth should variations of radius of curvature be with respect to the radius itself. Sensitivity to these variations depends on fiber specifications and are expressed through the adiabaticity curve. What the graph does not show is the concept of length. For instance, consider a point travelling at constant speed on a coil. The speed at which that point would travel on the adiabaticity curve would be variable. On the sequence of figuresof adiabaticity curves in this paper, the trajectories are repesented with dots. These dots are equally spaced on the coil itself. Therefore, one can evaluate distance on the adiabaticity graph by the density of dot in a given region. Though it is not the proper tool to evaluate absolute value of coupling, it does give a significant insight on the impact of coupling of a given coil geometry.

Few typical features are commonly present on these graphs. For instance, a straight piece of fiber is a dot at $(0, \infty)$. Bending a straight piece of fiber will bring the point from $(0, \infty)$ to (∞, ∞) and then down to the value of the radius itself. If the radius of curvature is then constant, the curve will go down to $(R_0, 0)$.

Perhaps the simpler case to study in appearance is the single round coil. However the information is less valuable from a point of view of trajectory on the adiabaticity graph. The theoritical shape is a straight piece of fiber, a coil of constant radius then a straight piece of fiber. On the trajectory graph, it would appear like a vertical line at $R = \infty$, a very high (but instantenous) value of ρ_0, and a vertical line at $R = R_0$, R_0 being the radius of curvature of the coil. As seen on figures 5 and 6, the impact of bending on coupling come from the approach to the fiber coil. As one can see on figures 7 and 8, a significant gain can be obtained by smoothing approach to a tight coil. The trade-off is obviously a slight increase in footprint.

The 8 shape coil presented on figures 9 and 10 was made with similar radius of coiling as the circular coil. However, while on the circular coil the trajectory was going from point (∞, ∞) to $(R_0, 0)$ and than back to (∞, ∞), the 8 shape coil does

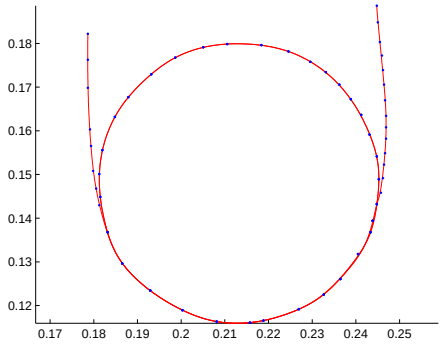

Figure 5. Path taken by a fiber in a circular coil. Dots are the experimental points taken on a picture. The line is the interpolation by cubic splines that is analysed on the adiabaticity curves.

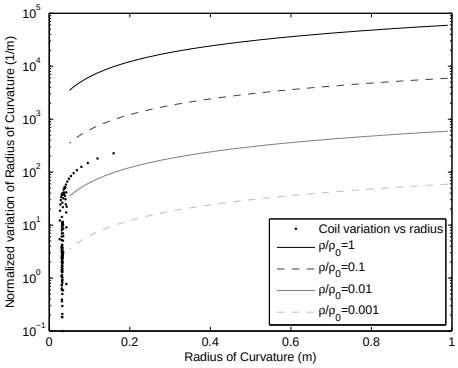

Figure 6. Trajectory on the adiabaticity curves of the circular coil.

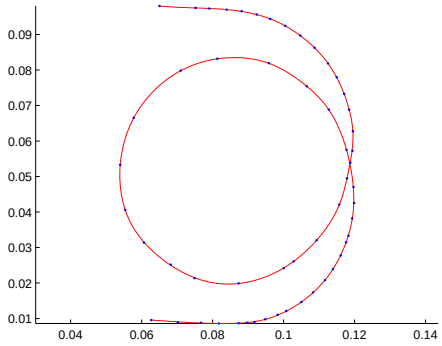

Figure 7. Path taken by a fiber in a smoothed approach simple coil. Dots are the experimental points taken on a picture. The line is the interpolation by cubic splines that is analysed on the adiabaticity curves.

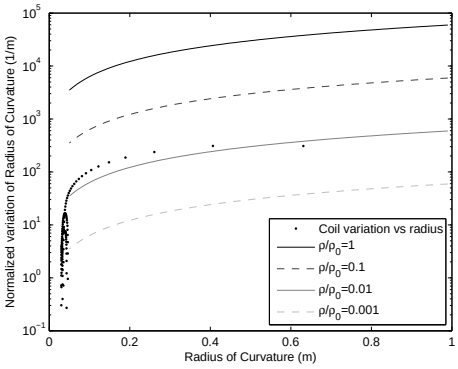

Figure 8. Trajectory on the adiabaticity curves of the smoothed approach simple coil.

the same, but repetitively. Here again, the vertical trajectories that goes down to small normalized variation of curvature are due to constant radius region of coiling. Even if small, those do not contribute in significant manner to LP_{01} to LP_{11} modal transfer, but the change of radius toward inflexion points does contribute. One can refer to figure 11 to follow radius of curvature and normalized variation of radius of curvature along the trajectory on a coil turn.

On adiabaticity curves, inflexion points are in the upper right part of the figure, which is big radius of curvature and rapid rate of change. One can see that the 8 shape coil has a smoother trajectory near the inflexion point, while the kidney shape coil changes the sign of radius of curvature while keeping a low absolute value of radius. Consequently, the kidney shape coil is significantly less adiabatic around the inflexion compared to 8 shape coil.

Interpretation of modal coupling has to be made carefully. One must not get confused with typical bending loss mechanism due to stress-induced variation of refractive index[4]. In this paper, only the coupling mechanism between modes is taken into account and not the coiling loss mechanism. A way to confirm presence of coupling mechanism is through appearance of transmission fringes as seen on figure 14. Fringes come from the fact that on constant piecewise radius coils, the coupling from LP_{01} to LP_{11} occurs at relatively non-adiabatic transition from straight to bent fiber or vice-versa and a phase shift is built between LP_{01} and LP_{11} in coiled sections. These are clearly seen for single coil and 8 shape coil transmission on figure 14. However, for the kidney shape coil, coupling still occurs as transitions are not adiabatic. However, the non-uniformity of bend radius through the coil acts as phase scrambler so the contrast of the interferometer fades but the power transfer still takes place. Finally, the smoothed approach single coil fiber had less cross-coupling, so less contrast with lower power transfer.

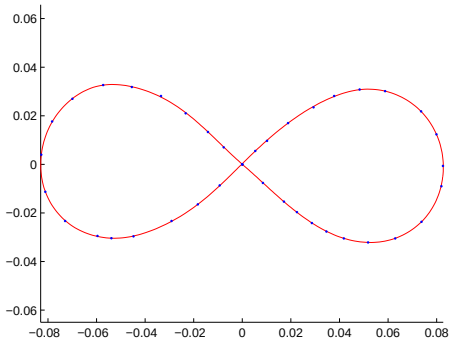

Figure 9. Path taken by a fiber in a 8 shape coil. Dots are the experimental points taken on a picture. The line is the interpolation by cubic splines that is analysed on the adiabaticity curves.

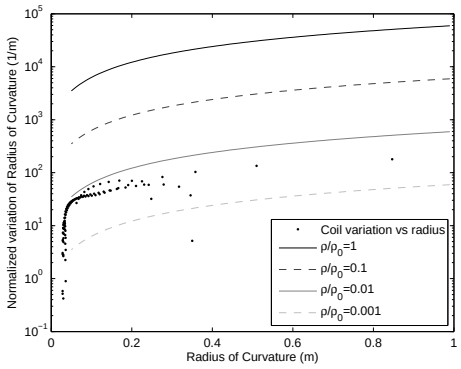

Figure 10. Trajectory on the adiabaticity curves of the 8 shape coil.

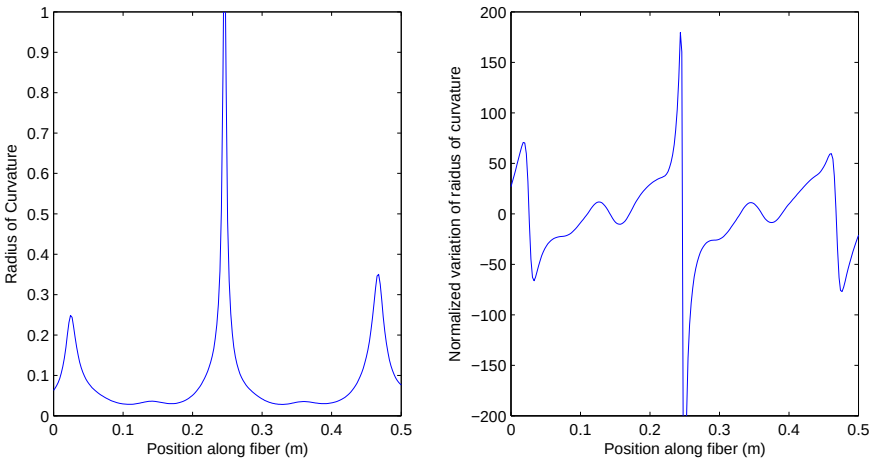

Figure 11. 8-shaped coil geometric study: Evolution of the radius of curvature and the normalized variation of radius of curvature. Due to numerical stability conisderations, the starting point was chosen to be just before the first inflexion point. A complete turn was considered and the end point was set just after passing again the fisrt inflexion point. Therefore, on the graph to the left, we see three peaks, the center one being the the second inflexion point, while the two other peaks represent the first inflexion point. The worst region for adiabaticity is local peaks on the graph to the right that match valleys on the left graph.

Note that there is a direct link between power transfer to higher order modes and beam quality. The way to preserve good beam quality is either by avoiding coupling by adiabatic coiling or by operating system on a wavelength that is on a peak transmission on a coil that exhibits spectral fringes.

6. CONCLUSION

In this article, we defined a new criterion for coiling adiabaticity. We also showed that while fiber takes a path that tends to distribute constraints, it minimizes variation of radius of curvature then giving good conditions for adiabatic coiling. The proposed model is of good use to design well-behaving coiled system, but has to be used in conjunction with other tools and constraints. The main limit to the model is the lack of capability in integrating punctual perturbation of coiling (local bending of the fiber).

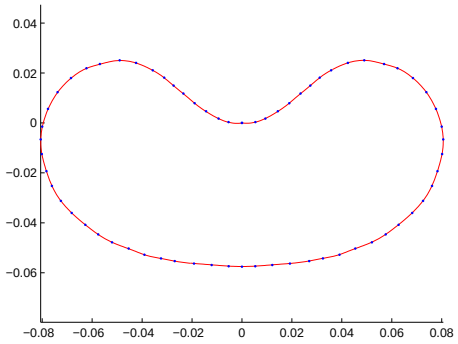

Figure 12. Path taken by a fiber in a kidney shape coil. Dots are the experimental points taken on a picture. The line is the interpolation by cubic splines that is analysed on the adiabaticity curves.

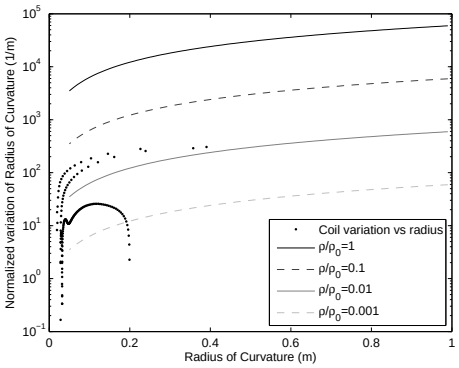

Figure 13. Trajectory on the adiabaticity curves of the kidney shape coil.

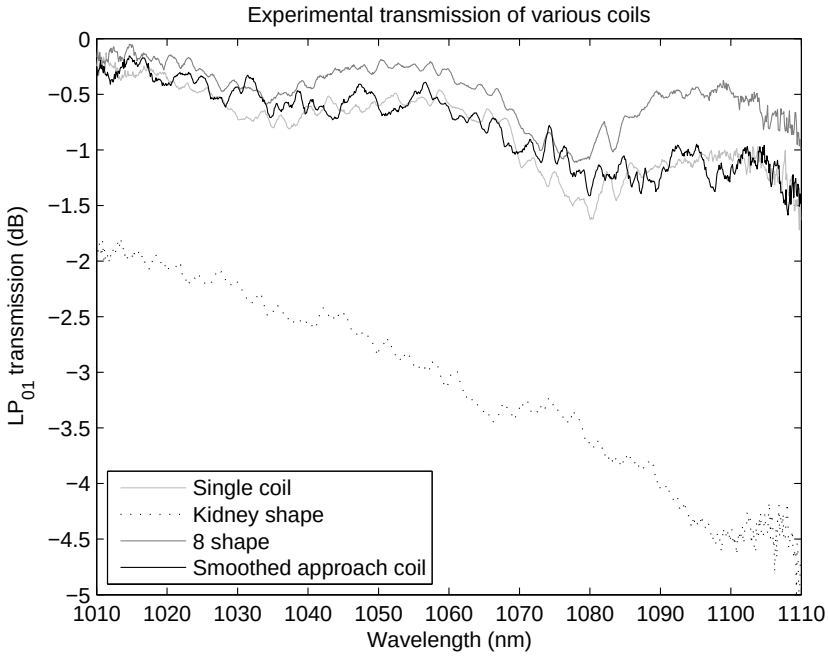

Figure 14. Various coil transmission spectrum. One can see that spectral oscillations are present in single coil and 8-shape coil. On the coil with smoothed approach, the oscillation amplitude is greatly reduced, but still visible. The kidney shape coil sees no oscillation, but significant losses.

REFERENCES

[1] B. Sévigny, X. Zhang, M. Garneau, M. Faucher, Y. K. Lizé, and N. Holehouse, "Modal sensitivity analysis for single mode operation in large mode area fiber," *Fiber Lasers V: Technology, Systems, and Applications* **6873**(1), p. 68730A, SPIE, 2008.

[2] H. Hamam, ed., *Optical Fiber Components: Design and Applications*, Research Signpost, 2006.

[3] K. Meerbergen, A. Spence, and D. Roose, "Shift-invert and cayley transforms for detection of rightmost eigenvalues of nonsymmetric matrices," *BIT Numerical Mathematics* **34**(3), pp. 409–423, 1994.

[4] R. T. Schermer, "Mode scalability in bent optical fibers," *Opt. Express* **15**(24), pp. 15674–15701, 2007.